Dextrous Manipulation with Rolling Contacts

L. Han TAMU   Y.S. Guan HKUST   Z.X. Li* HKUST   Q. Shi HKUST   J.C.Trinkle † TAMU

Abstract

Dextrous manipulation is a problem of paramount importance in the study of multifingered robotic hands. Given a grasped object, the main objectives are: (a) generate trajectories for the finger joints so that through the effects of contact constraints, the object can be transferred to a goal grasp configuration; and (b) derive control algorithms to realize planned trajectories. In this paper, we integrate the relevant theories of contact kinematics, nonholonomic motion planning and grasp stability to develop a general technique for dextrous manipulation planning with multifingered hands. Experimental results are discussed.

1 Introduction

Given an object to be manipulated by a robotic hand, the goal of dexterous manipulation planning algorithms is to generate finger joint trajectories that can drive the object to the desired configuration while simultaneously achieving the desired grasp. Various aspects of the dexterous manipulation problem have been studied by many researchers over the past 15 years[9] but a solution to the general problem[2] remains elusive.

In this paper, we take a step toward a general solution by integrating the relevant theories of contact kinematics[6], nonholonomic motion planning[2] [7], and grasp stability[8] to develop a general technique for dexterous manipulation with multifingered robotic hands. To simplify the presentation we consider only the special, but important case, of a flat fingertip rolling a ball on a plane. We derive in detail, the relevant relations needed to formulate dexterous manipulation planning problem, cast them in a form suitable for execution by a robotic hand, and present experimental results. The experiments were performed with the HKUST hand system (see figure 1).

Figure 1: The HKUST robotic hand.

2 Mathematical Preliminaries

This section provides a brief introduction to kinematics. See[7] for a detailed discussion.

2.1 Rigid Body Kinematics

A configuration of a frame B relative to another frame A is given by an element g_{ab} of the special Euclidean group, $SE(3)$, and has the form

$$g_{ab} = \begin{bmatrix} R_{ab} & p_{ab} \\ 0 & 1 \end{bmatrix}$$

where $R_{ab} \in SO(3)$ represents orientation and $p_{ab} \in \Re^3$ represents translation of B relative to A. The body velocity of B relative to A is defined using left translation given by

$$\widehat{V}_{ab} = g_{ab}^{-1}\dot{g}_{ab} = \begin{bmatrix} R_{ab}^T\dot{R}_{ab} & R_{ab}^T\dot{p}_{ab} \\ 0 & 0 \end{bmatrix} = \begin{bmatrix} \hat{\omega}_{ab} & v_{ab} \\ 0 & 0 \end{bmatrix} \quad (1)$$

where for $\omega = (\omega_1, \omega_2, \omega_3)$, $\widehat{\omega} \in so(3)$. $V_{ab} = (v_{ab}, \omega_{ab}) \in \Re^6$ is also known as the generalized (body) velocity of B relative to A.

Given three coordinate frames, A, B and C, their relative velocities are related by

$$V_{ac} = Ad_{g_{bc}^{-1}} V_{ab} + V_{bc} \quad (2)$$

---

*Electrical and Electronic Engineering Dept., Hong Kong University of Science and Technology, clear water bay, Hong Kong. Research supported in part by RGC Grant No. HKUST 685/95E, HKUST 555/94E and HKUST 193/93E. Special thanks go to Z Qin, S Jiang and T. Choi for their assisatnce in the experiments and useful discussions on part of the paper.

†Computer Science Dept., Texas A&M University, College Station, Texas 77843-3112. This research was supported in part by NSF grant no. IRI-9304734 and Amarillo National Resource Center for Plutonium grant number UTA95-0278.

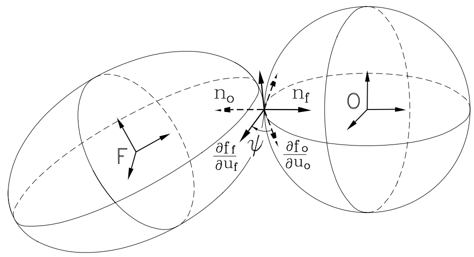

Figure 2: Motion of two objects in contact

where for $g = (p, R) \in SE(3)$, the adjoint transformation Ad_g is defined by $Ad_g = \begin{bmatrix} R & \widehat{p}R \\ 0 & R \end{bmatrix} \in \mathrm{R}^{6\times 6}$

2.2 Kinematics of Contact

We parameterize the surface of a smooth object by a differentiable map

$$f : U \subset \Re^2 \to \mathrm{R}^3, \quad \alpha = (u, v) \longmapsto f(\alpha).$$

We assume that f is orthogonal, i.e., $f_u \cdot f_v = 0$, and right-handed, i.e. $n = \frac{f_u \times f_v}{\|f_u \times f_v\|}$ coinciding with the unit outward surface normal. At each point of contact we define the Gauss frame C by $g_{oc} = (p_{oc}, R_{oc})$ with $p_{oc} = f(\alpha)$ and

$$R_{oc} = \begin{bmatrix} x & y & z \end{bmatrix} = \begin{bmatrix} \frac{f_u}{\|f_u\|} & \frac{f_v}{\|f_v\|} & \frac{f_u \times f_v}{\|f_u \times f_v\|} \end{bmatrix}.$$

In terms of the Gauss frame, we denote by M, K, and T, the *metric tensor*, the *curvature tensor*, and the *torsion form* of the surface[7].

Suppose that two objects F and O are in contact at a point p (See Figure 2). We let $\alpha_f = (u_f, v_f)$ and $\alpha_o = (u_o, v_o)$ be the local coordinates of F and O, respectively, ψ the angle of contact, and denote the contact coordinates by $\eta = (\alpha_f, \alpha_o, \psi)$.

Denote the metric and curvature tensors and torsion forms of F and O by (M_f, K_f, T_f) and (M_o, K_o, T_o), respectively. Let L_f and L_o be the local frames of F and O which coincide with the Gauss frames at the moment of contact and fixed relative relative to F and O respectively. Denote the contact velocity of F relative to O in terms of their local frames by

$$V_c = V_{of}^{l_f} = [v_{of}^{l_f}, \omega_{of}^{l_f}]^T = [v_x,\ v_y,\ v_z,\ \omega_x,\ \omega_y,\ \omega_z]^T.$$

The kinematic velocity constraints associated with pure rolling contact are: $v_z = v_x = v_y = \omega_z = 0$.

The kinematic equations of contact relating the two components of rolling velocities (ω_x, ω_y) to the rate of change of the contact coordinates are given by [6]

$$\begin{cases} \dot{\alpha}_f = M_f^{-1}(K_f + \tilde{K}_o)^{-1} \begin{bmatrix} -\omega_y \\ \omega_x \end{bmatrix} \\ \dot{\alpha}_o = M_o^{-1} R_\psi (K_f + \tilde{K}_o)^{-1} \begin{bmatrix} -\omega_y \\ \omega_x \end{bmatrix} \\ \dot{\psi} = T_f M_f \dot{\alpha}_f + T_o M_o \dot{\alpha}_o \end{cases} \quad (3)$$

where $R_\psi = \begin{bmatrix} cos\psi & -sin\psi \\ -sin\psi & -cos\psi \end{bmatrix}$ and $\tilde{K}_o = R_\psi K_o R_\psi$ is the curvature of O seen in the local frame of F.

2.3 Nonholonomic Motion Planning

A nonholonomic motion planning system is described by a driftless nonlinear control system of the form

$$\dot{q} = g_1(q)u_1 + \cdots + g_m(q)u_m \quad (4)$$

where $q \in \mathrm{R}^n$ represents the states, $u = (u_1, \cdots u_m), m < n$, represents the control inputs, and $(g_1(q), \cdots g_m(q))$ defines a nonholonomic distribution in the configuration space of the system. Given two configurations q_0 and q_f, the study of nonholonomic motion planning amounts to finding optimal inputs $u : [0, T] \to \mathrm{R}^m$ so that the solution of (4) connects q_0 to q_f. In our context, the equations of (3) give rise to a nonholonmomic motion planning system if we treat $(\omega_x, \omega_y) = (u_1, u_2)$ as the control inputs. The nonholonomic distribution associated with the system can be derived using the geometric parameters of the contacting bodies. To change contact configurations with rolling constraint, we simply let the two components of rolling velocities be the control inputs and solve the corresponding nonholonomic motion planning problem. A solution technique using geometric phases is discussed in [2] and other more general techniques can be found in [3] and [7].

3 Dexterous Manipulation: Rolling a Ball on a Plane

For the case of a flat fingertip rolling an object (a ball) on a palm (a plane) as shown in Figures 3 and 5, our objective of the manipulation planing is to determine the finger joint trajectory, so that through the effects of contact constraints we: (1) achieve the goal configuration of the object(ball), and simultaneously (2) improve the grasp quality.

Let P, F and O be, respectively, the reference frame of the palm, finger and object. Parameterize the fingertip and the palm using flat coordinates, and the ball using longitude and latitude angles, we can derive the geometric parameters of the fingertip, the palm, and the ball [7].

Let $\eta_f = (\alpha_f, \alpha_{of}, \psi_f)$ be the coordinates of contact between the finger and the object, and $\eta_p =$

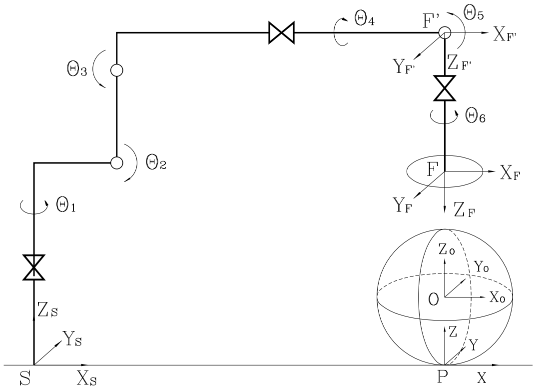

Figure 3: Diagram of finger and frame specification

$(\alpha_p, \alpha_{op}, \psi_p)$ the coordinates of contact between the object and the palm, and $\theta_f \in \Re^m, m \le 6$, the joint angles of the finger. A grasp configuration of the system is defined by $\Theta = (\theta_f, \eta_f, \eta_p)$.

By viewing the system as a closed kinematic chain, Θ satisfies the so-called closure constraint [6] and also physical constraints imposed by rolling contact. We can use the resulting constraint equations to do dexterous manipulation planning in a general approach [1]. But, because of the kinematic simplicity of the system it is more convenient to do so as follows. First, the forward kinematics of the finger gives the velocity of F in terms of the joint rates as

$$V_{pf} = J_f(\theta_f)\dot{\theta}_f. \tag{5}$$

Thus, if V_{pf} is specified, then we can solve for the desired joint rates from (5) using either the pseudo inverse or generalized inverse of J_f and feed the results to the finger controller.

On the other hand, Figure 3 implies the following constraint holds

$$g_{pf} = g_{po} g_{oc_{o_f}(\alpha_{o_f})} g_{c_{o_f}c_f(\psi_f)} g_{c_f f(\alpha_f)} := g_{po} g_{of(\eta_f)} \tag{6}$$

where C_f and C_{o_f} are, respectively, the Gauss frame of the finger and the object at the point of contact. Differentiating (6) gives the velocity relation

$$V_{pf} = Ad_{g_{of}^{-1}}(\eta_f) V_{po} + J_{of}(\eta_f)\dot{\eta}_f \tag{7}$$

where J_{of} is the Jacobian of the second term in (6). Next, we use nonholonomic motion planning and optimization of a grasp quality measure to specify the right hand side of (7).

One objective of dexterous manipulation is to change contact state η_p from η_p^0 to η_p^f, and thus, implicitly change the object from its initial configuration to goal configuration. Because of the rolling constraint, we pose this as a nonholonomic motion planning problem with input $(u_1, u_2) = \dot{\alpha_p}$. Substituting this into the kinematic equations of contact for η_p we obtain

$$\dot{\eta}_p = g_1(\eta_p)u_1 + g_2(\eta_p)u_2 \tag{8}$$

where

$$g_1(\eta_p) = \begin{bmatrix} 1 & 0 & \frac{1}{\rho_0} c_{\psi_p} & -\frac{1}{\rho_o}\frac{s_{\psi_p}}{c_{u_{op}}} & \frac{1}{\rho_0} s_{\psi_p} t_{u_{op}} \end{bmatrix}^T,$$

$$g_2(\eta_p) = \begin{bmatrix} 0 & 1 & -\frac{1}{\rho_o} s_{\psi_p} & -\frac{1}{\rho_o}\frac{c_{\psi_p}}{c_{u_{op}}} & \frac{1}{\rho_o} c_{\psi_p} t_{u_{op}} \end{bmatrix}^T.$$

Techniques from nonholonomic motion planning can be applied to (8) to solve for u or $\dot{\alpha}_p$. Once $\dot{\alpha}_p$ is found, the two components of rolling velocities are given by

$$\begin{bmatrix} -\omega_{py} \\ \omega_{px} \end{bmatrix} = K_o R_{\psi_p} \dot{\alpha}_p.$$

Given $(-\omega_{py}, \omega_{px})$, the velocity of the object is completely determined:

$$V_{po} = Ad_{g_{ol_p}} B \begin{bmatrix} -\omega_{py} \\ \omega_{px} \end{bmatrix} \tag{9}$$

where $B^T = \begin{bmatrix} 0 & 0 & 0 & 0 & -1 & 0 \\ 0 & 0 & 0 & 1 & 0 & 0 \end{bmatrix}$.

With V_{po} determined, we next specify $\dot{\eta}_f$ to determine V_{pf}. Again, because of rolling constraints, $\dot{\eta}_f$ is uniquely determined by $\dot{\alpha}_{of}$. We choose $\dot{\alpha}_{of}$ so as to optimize a quality of the grasp, and this constitutes the second objective of dexterous manipulation.

Referring to figure 4(a), let n_p and n_f be the outward surface normal of the object at the point of contact with the palm and the finger, respectively.

Let $g_{l_{op}l_{of}} = g_{ol_{op}}^{-1} g_{ol_{of}} := \begin{bmatrix} R_0 & P_0 \\ 0 & 1 \end{bmatrix}$,

Then, $n_p = \begin{bmatrix} 0 \\ 0 \\ 1 \end{bmatrix}$, $\quad n_f = R_0 \begin{bmatrix} 0 \\ 0 \\ 1 \end{bmatrix}$

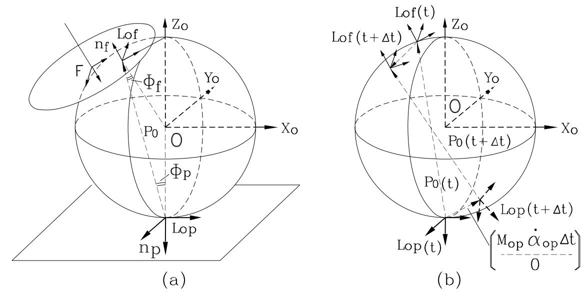

Figure 4: Grasp Angles and change of contact

Define two *grasp angles* [5] by

$$\Phi_p := cos^{-1}(-n_p \bullet \frac{p_0}{||p_0||}); \quad \Phi_f := cos^{-1}(n_f \bullet \frac{p_0}{||p_0||}).$$

The grasp is force closure [8] if

$$max(\Phi_p, \Phi_f) < tan^{-1}(\mu)$$

where μ is the Comlumb friction coefficient.

Assume that α_{op} and α_{of} undergo infinitesimal displacement during time interval $[\ t,\ t+\Delta t\ ]$, then,

$$\alpha_{op}(t) \mapsto \alpha_{op}(t+\Delta t) = \alpha_{op}(t) + \dot{\alpha}_{op}(t)\Delta t;$$

$$\alpha_{of}(t) \mapsto \alpha_{of}(t+\Delta t) = \alpha_{of}(t) + \dot{\alpha}_{of}(t)\Delta t.$$

Relative to L_{op}, we have

$$\begin{aligned} n_p(t+\Delta t) &= R_{l_{op}o}(t) R_{ol_{op}}(t+\Delta t) \begin{bmatrix} 0 \\ 0 \\ 1 \end{bmatrix} \\ &= R^T_{ol_{op}}(t) \begin{bmatrix} -c_{u_{op}(t+\Delta t)} s_{v_{op}(t+\Delta t)} \\ -s_{u_{op}(t+\Delta t)} \\ -c_{u_{op}(t+\Delta t)} c_{v_{op}(t+\Delta t)} \end{bmatrix} \end{aligned}$$

$$n_f(t+\Delta t) = R_0 R^T_{ol_{of}}(t) \begin{bmatrix} -c_{u_{of}(t+\Delta t)} s_{v_{of}(t+\Delta t)} \\ -s_{u_{of}(t+\Delta t)} \\ -c_{u_{of}(t+\Delta t)} c_{v_{of}(t+\Delta t)} \end{bmatrix}$$

$$P_0(t+\Delta t) = P_0 + R_0 \begin{bmatrix} M_o \dot{\alpha}_{of} \Delta t \\ 0 \end{bmatrix} - \begin{bmatrix} M_o \dot{\alpha}_{op} \Delta t \\ 0 \end{bmatrix}$$

The grasp angles change to:

$$\Phi_p(t+\Delta t) = cos^{-1}(-n_p(t+\Delta t) \bullet \frac{P_0(t+\Delta t)}{||P_0(t+\Delta t)||})$$

$$\Phi_f(t+\Delta t) = cos^{-1}(n_f(t+\Delta t) \bullet \frac{P_0(t+\Delta t)}{||P_0(t+\Delta t)||}).$$

Define the *objective function* to be minimizing

$$F_1(\dot{\alpha}_{of}) = max(\Phi_p(\dot{\alpha}_{of}), \Phi_f(\dot{\alpha}_{of})).$$

To achieve good grasp quality, we choose $\dot{\alpha}_{of}$ to minimize the function F_1 subject to the constraint of rotation. The angle of relative rotation is:

$$\begin{aligned} \begin{bmatrix} -\Delta\Theta_{f_y} \\ \Delta\Theta_{f_x} \end{bmatrix} &= \begin{bmatrix} -\omega_{f_y} \\ \omega_{f_x} \end{bmatrix} \Delta t \\ &= (K_f + \tilde{K}_{of})^{-1} R_{\psi_f} M_o \dot{\alpha}_{of} \Delta t \\ &= R_{\psi_f} K_o^{-1} M_o \dot{\alpha}_{of} \Delta t. \end{aligned}$$

We define the *constraint function* to be

$$F_2(\dot{\alpha}_{of}) = ||\Delta\Theta(\dot{\alpha}_{of})|| < \delta \quad (\delta > 0). \qquad (10)$$

To minimize F_1 subjective to (10), we rewrite the constraint as

$$A \begin{bmatrix} \Delta\Theta_{f_x} \\ \Delta\Theta_{f_y} \end{bmatrix} = \dot{\alpha}_{of}$$

where

$$A = \frac{1}{\Delta t} M_o^{-1} K_o R_{\psi_f} \begin{bmatrix} 0 & -1 \\ 1 & 0 \end{bmatrix}.$$

Let the singular value decomposition of A be

$$A = U \begin{bmatrix} \sigma_1 & 0 \\ 0 & \sigma_2 \end{bmatrix} V^T.$$

Then, A takes a unit ball to an ellipsoid with principal axes $U = (u_1, u_2)$ and of length σ_1 and σ_2.

We use a grid-based search in an ellipsoid of size δ to find solution of the constrained optimization problem. The results are then used to compute $\dot{\eta}_f$ and consequently V_{pf}.

4 Dexterous Manipulation: Two Flat Fingertips Manipulating a Ball

It is natural to generalize the technique developed in the previous section to the case of two flat fingertips manipulating a ball (see Figure 8).

Let η_{f1} and η_{f2} be the coordinates of contact of the object with finger 1 and finger 2, respectively. Let θ_1 and θ_2 be the joint angles of finger 1 and finger 2. A grasp configuration of the system is given by $\Theta = (\theta_1, \theta_2, \eta_{f1}, \eta_{f2})$.

By viewing the system as a closed kinematic chain we can derive the closure constraint as well as the physical constraints imposed by rolling contacts. Utilizing these constraints, we define the two objectives of dexterous manipulation to be: (a) tracking a desired trajectory of the object, and (b) optimizing the quality of a grasp. The development to compute the desired inputs for the joint angles of the fingers is similar to that of Section 3, see [4] for more details.

5 Experimental Results

In this section, we present experimental results obtained by implementing the results from Section 3 and 4 on the HKUST hand system.

5.1 HKUST Hand System

Using three modified Motoman K3S robots, we recently developed a three-fingered robotic hand (see Figure 1) as our research platform for study of dexterous manipulation. The HKUST hand is easily reconfigurable in terms of the base configuration, the geometries of the fingertips and the numbers of degree-of-freedom of the fingers. A spherically shaped fingertip and a flat fingertip have been designed for each finger. Also, by locking some of the joints of the six

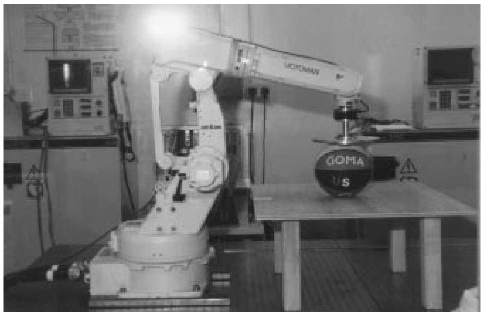

Figure 5: A flat fingertip rolling a ball on a plane

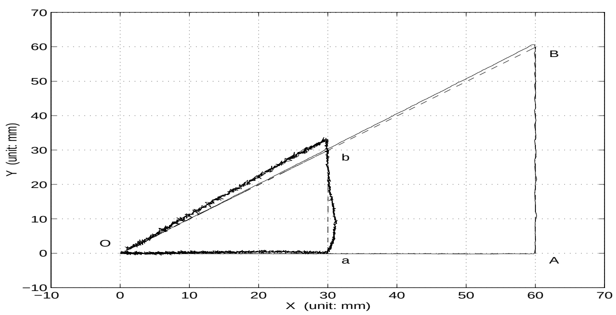

Figure 6: Trajectories of the ball and the fingertip

DOF fingers we can make them look more like "ordinary" fingers.

Sensors built into the HKUST hand include joint position sensors from encoder readings, a force/torque sensor at the nearest end of the fingertip and a 16×16 tactile sensor array mounted to the fingertip. Based on a point contact model assumption, the force/torque sensor can be used to measure both contact force and contact locations [10] [11], which is the case in our experiments.

5.2 Experiment Results

We have done a number of experiments in which we manipulated the ball to follow a desired trajectory, such as rotating the ball about any axis, and translating the ball along any given direction, while the trajectories of the contact coordinates were chosen so as to optimize the quality of the grasp. For brevity, we only present the following two experiment results:

(1) For the case of one flat fingertip rolling a ball on a plane (figure 5), the initial conditions are: $\theta = (\ 0,\ -22.68,\ -12.34,\ 0,\ 47.65,\ 0\ )$, $\eta_f = (\ 0,\ 0,\ 0,\ 0,\ 0\ )$, $\eta_p = (\ 0,\ 0,\ 0,\ 0,\ -90^o\ )$. We chose a path for the contact point on the palm $\alpha_p(t)$ to be a triangle specified by three points (0, 0), (30, 0) and (30, 30).

In Figure 6, the dashed line *oabo* and *OABO* are desired trajectories of the ball center and the fingertip, respectively. The jagged solid line *oabo* and *OABO* are the actual trajectories of the ball and the fingertip. Note that the ball's center was computed using tactile sensor reading and the relationships developed in Section 2.

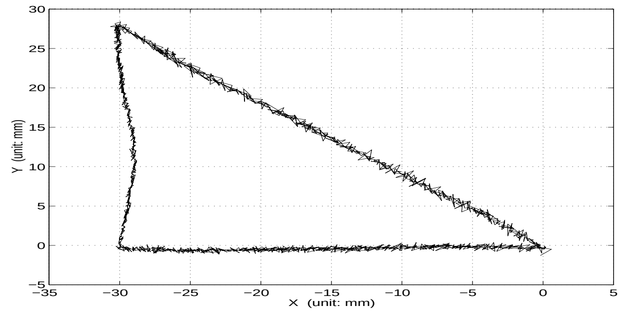

Figure 7: Localization of the contact point across the fingertip

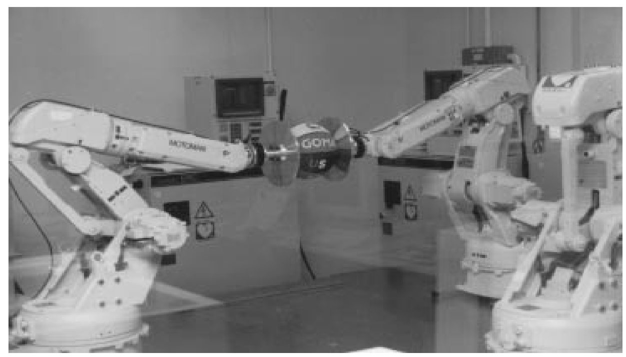

Figure 8: A two-fingered robot hand with flat fingertips manipulating a ball

Figure 7 displays the trajectory of contact relative to the fingertip computed using the force/torque sensor readings. The resolution of the results were found to be less than $2mm$, which is quite satisfactory compared with that of the tactile array.

Note that in this case the optimal grasp should be antipodal, i.e., the contact between the fingertip and the ball should be at the "north pole". In the experiment, we purposely chose initial conditions to be different from that of the optimal value. Using the optimization algorithm, we found the grasp to quickly converge to the optimal value.

(2) For the case of two flat fingertips manipulating a ball(figure 8). The desire trajectory is to rotate the ball first about the Z-axis for 20^o, then Y-axis for 20^o, then Z-axis for -20^o and then Y-axis for -20^o. The experiment results are show in figures 9 and 10.

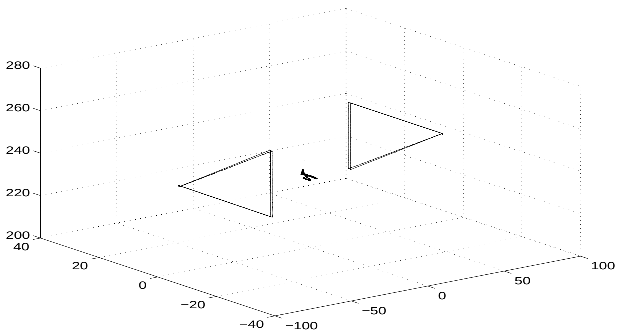

Figure 9: Trajectories of ball and fingertips: X, Y and Z direction

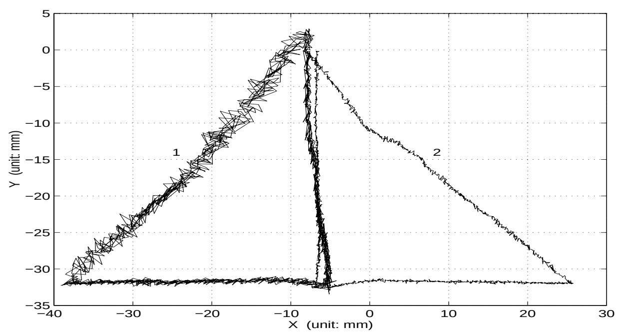

Figure 10: Localization of contact points on fingertips

6 Conclusion

In this paper, by integrating the relevant theories of contact kinematics, nonholonomic motion planning, and grasp stability, we developed a general technique for dexterous manipulation with multifingered robotic hands. The detailed kinematic relations and precise formulation of the problem of dexterous manipulation in the case of a flat fingertip rolling a ball on a plane were derived. While nonholomic motion planning techniques were used to generate desired trajectories of the ball, the coordinates of contact between the finger and the object were chosen so as to optimize the quality of the grasp. The experimental results for this case as well as the case of two flat fingers manipulating a ball using the HKUST hand system were presented. Currently, we are conducting experimental studies on dexterous manipulation with a three-fingered robotic hand with both rolling contact and finger gaiting.

References

[1] L. Han and J.C. Trinkle. Theorey and experiments of dextrous manipulation. Technical report, Computer Science, Texas A & M Univ., 1996.

[2] Z. Li and J. Canny. Motion of two rigid bodies with rolling constraint. *IEEE Trans. on R. & A.*, RA2-06:62–72, 1990.

[3] Z. X. Li and J. Canny, editors. *Nonholonomic Motion Planning.* Kluwer Academic Publisher, 1993.

[4] Z.X. Li, Q. Shi, Y. Guan, S. Jiang, and Z. Qin. Fundamentals of multifingered robotic hand manipulation: Theory and experiments. Technical report, Hong Kong Univ. of Science and TEchnology, 1996.

[5] D. Montana. The kinematics of contact and grasp. *IJRR*, 7(3), 1988.

[6] D. Montana. The kinematics of multi-fingered manipulation. *IEEE Trans. on R. & A.*, 11(4):491–503, 1995.

[7] R. Murray, Z.X. Li, and S. Sastry. *A Mathematical Introduction to Robotic Manipulation.* CRC Press, 1994.

[8] V. Nguyen. The synthesis of force-closure grasps. Master's thesis, Department of Electrical Engineering and Computer Science, MIT, 1986.

[9] J. Pertin-Troccaz. Grasping: A state of the art. In O. Khatib, J. J. Craig, and T. Lozano-Pérez, editors, *The Robotics Review I*, pages 71–98. MIT Press, 1989.

[10] J. Son, M. Cutkosky, and R. Howe. Comparison of contact sensor localization abilitities during manipulation. In *Proc. of IEEE Intl. Conf. on Robotics and Automation*, pages 96–103, 1995.

[11] X.C. Zhou, Q. Shi, and Z. X. Li. Contact localization using force/torque measurement. In *IEEE Intl. Conf. on Robotics and Automation*, 1996.